Regiospecificity Assignment for the Reaction of Kanamycin Nucleotidyltransferase from *Staphylococcus aureus*[†]

Barbara Gerratana, W. W. Cleland, and Laurie A. Reinhardt*

Institute for Enzyme Research, Department of Biochemistry, College of Agricultural Life Sciences, University of Wisconsin−Madison, Madison, Wisconsin 53705

Received November 6, 2000; Revised Manuscript Received January 17, 2001

ABSTRACT: Aminoglycoside nucleotidyltransferases catalyze the transfer of a nucleoside monophosphoryl group from a nucleotide to a hydroxyl group of an aminoglycoside antibiotic. Kanamycin nucleotidyltransferase [ANT (4′,4″)-I] from *Staphylococcus aureus* confers resistance to numerous aminoglycosides with a 4′ or 4″ hydroxyl group in the equatorial position. The synthesis of *m*-nitrobenzyl triphosphate, a new substrate of kanamycin nucleotidyltransferase, is reported. The kanamycin nucleotidyltransferase catalyzed reaction of kanamycin A with *m*-nitrobenzyl triphosphate is 2 orders of magnitude slower than that with ATP. The MALDI-TOF spectra of the purified products of both reactions revealed that kanamycin A was modified only at one position. The regiospecificity of the reaction catalyzed by kanamycin nucleotidyltransferase of kanamycin A with either ATP or *m*-nitrobenzyl triphosphate was determined directly by one- and two-dimensional hetero- and homonuclear NMR techniques. The site of the modification was unambiguously assigned to the 4′ hydroxyl of kanamycin A; thus, the products formed are 4′-(adenosine-5′-phosphoryl)-kanamycin A and 4′-(*m*-nitrobenzyl phosphoryl)-kanamycin A. This eliminates the uncertainty concerning the point of modification since this could not be determined from the crystal structure of the enzyme with bound MgAMPCPP and kanamycin A [Pedersen, L. C., Benninig, M. M., and Holden, H. M. (1995) *Biochemistry 34,* 13305−13311].

The natural or semisynthetic aminoglycosides are antimicrobial agents containing a central aminocyclitol moiety with one or more aminosugars linked to it. Since their approval for clinical use, aminoglycosides have been very effective in treating bacterial diseases. However, in recent years an alarming number of staphylococci and enterococci have shown resistance to aminoglycoside antibiotics (*1*). The bactericidal effect of the aminoglycosides is caused by its binding to the bacterial 30S ribosomal subunit. The resulting inhibition of normal protein biosynthesis eventually leads to cell death (*2*). Extensive use of aminoglycosides in the treatment of bacterial infections has resulted in the development of new strains of resistant bacteria. Although resistance to the aminoglycosides is acquired through many different mechanisms, the most commonly found is the enzymatic inactivation of the drugs. Bacteria encode three main classes of aminoglycoside-inactivating enzymes, the *O*-phosphotransferases (APH), the *O*-nucleotidyltransferases (ANT), and the *N*-acetyltransferases (ACC) (*3*).

Aminoglycoside nucleotidyltransferases catalyze the transfer of a nucleoside monophosphoryl group from a nucleotide to a hydroxyl group of an aminoglycoside antibiotic. Two types of aminoglycoside 4′-nucleotidyltransferases are known: ANT (4′,4″)-I from Gram positive bacteria and ANT (4′)-II from Gram negative bacteria (*4*). Aminoglycoside 4′-nucleotidyltransferases from Gram positive bacteria are able to nucleotidylate aminoglycoside antibiotics that contain a 4′ or 4″ hydroxyl group in the equatorial position. Thus, 3′,4′-dideoxykanamycin B (dibekacin), which lacks a 4′ target but has a 4″ equatorial hydroxyl group, is a substrate for ANT (4′,4″)-I from *Staphyloccocus epidermis* (*5*).

Kanamycin nucleotidyltransferase[1] from the enzyme class ANT (4′,4″)-I was first isolated from *Staphylococcus aureus*. The enzyme confers resistance to a number of aminoglycosides which possess a 4′ hydroxyl in the equatorial position, but it does not modify aminoglycosides with a 4′ hydroxyl

[†] This work was supported by NIH Grant GM18938 to W.W.C. This study made use of the National Magnetic Research Facility at Madison, which is supported by NIH Grant RR02301 from the Biomedical Research Technology Program, National Center for Research Resources. Equipment in the facility was purchased with funds from the University of Wisconsin, the NSF Biological Instrumentation Program (Grant DMB-8415048), NIH Biomedical Research Technology Program (Grant RR02301), NIH Shared Instrumentation Program (Grant RR02781), and the U.S. Department of Agriculture.

* To whom correspondence should be addressed. Phone: (608) 262-5828. Fax: (608) 265-2904. E-mail: lareinha@facstaff.wisc.edu.

[1] Abbreviations: KNTase, kanamycin nucleotidyltransferase; TK1, D80Y KNTase mutant; KanA, kanamycin A; KanA-AMP, 4′-(adenosine-5′-phosphoryl)-kanamycin A; KanA-*m*NBMP, 4′-(*m*-nitrobenzyl phosphoryl)-kanamycin A; *m*NBTP, *m*-nitrobenzyl triphosphate; AMPCPP, adenosine 5′-α,*β*-methylenetriphosphate; TEAB, triethylammonium bicarbonate; TLCK, N_{α}-*p*-tosyl-L-lysine chloromethyl ketone; IPTG, isopropyl *β*-D-thiogalactopyranoside; PMSF, phenylmethanesulfonyl fluoride; NOE, nuclear Overhauser enhancement; TOCSY, total correlation spectroscopy; DEPT, distortionless enhancement by polarization transfer; HMQC-TOCSY, heteronuclear multiple-quantum coherence and total correlation spectroscopy; HSQC, heteronuclear single-quantum coherence spectroscopy; HMQC, heteronuclear multiple-quantum coherence spectroscopy; DFCOSYPS, double quantum filtered correlation spectroscopy phase sensitive; MALDI-TOF, matrix-assisted laser desorption time-of-flight mass spectrometry.

10.1021/bi0025565 CCC: $20.00
Published on Web 02/08/2001

Scheme 1

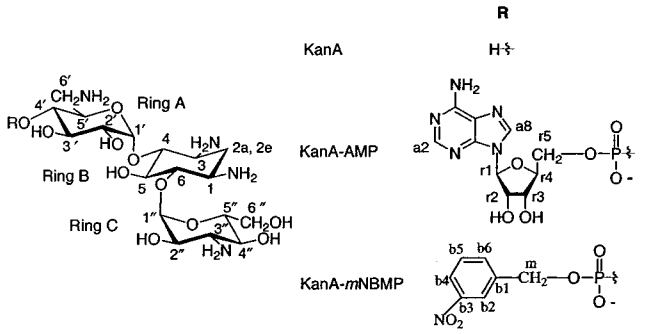

group in the axial position (*6*). A direct assignment of the regiospecificity of this KNTase reaction with KanA based on product analysis has not yet been reported. The crystal structure of the KNTase thermostable mutant D80Y (TK1) complexed with kanamycin A and the nonhydrolyzable nucleotide analogue AMPCPP has been solved at 2.5 Å (*7*). Unfortunately, due to the similarity in the chemical structures of rings A and C of kanamycin A (Scheme 1), it was not possible to ascertain from the difference in the electron density of the kanamycin A molecule the identity of the group pointing toward the α-phosphorus as the 4′ or the 4″ hydroxyl group in the active site (*7*).

The reaction of KNTase with KanA and ATP follows an ordered Bi−Bi mechanism with the release of the KanA-AMP as the rate-limiting step (*8*). The synthesis of a slow substrate analogue, *m*-nitrobenzyl triphosphate, and the kinetic characterization of the reaction of KNTase with ATP or with *m*NBTP is reported here. We investigate the regiospecificity of the reaction of KNTase with kanamycin A in the presence of ATP or *m*NBTP in order to assess whether one or both of the 4′ and 4″ hydroxyl groups of KanA are the site(s) of the aminoglycoside modification. The complete NMR assignments of KanA, KanA-AMP, and KanA-*m*NBMP were determined at neutral pH from a series of 1D and 2D NMR spectra. The site of the chemical modification of KanA in the reaction catalyzed by KNTase is the 4′ hydroxyl group with either ATP or *m*NBTP as the cosubstrate. These results led to the determination of the transition-state structure of the reaction of KNTase described in the following paper in this issue.

EXPERIMENTAL PROCEDURES

Materials. Butyl Sepharose FF and Sephacryl S200 resins were from Pharmacia, while all the other resins, chemicals and coupling enzymes were from Sigma. All the buffers were obtained from Aldrich. Plasmid pALT/TK1 was a generous gift from Prof. H. M. Holden, Department of Biochemistry, University of Wisconsin—Madison.

Mass Spectrometry of mNBTP, KanA-AMP, and KanA-mNBMP. MALDI-TOF mass spectra were collected on a Bruker Reflex II TOF-MS equipped with a N_2 laser. For spectra collected in the negative mode an accelerating voltage of 20.0 kV and a reflectron voltage of 21.20 kV were used. For spectra collected in the positive mode an accelerating voltage of 25 kV and a reflectron voltage of 26.50 kV were used. The matrix used for all experiments was α-cyano-4-hydroxycinnamic acid. Samples were prepared in the NH_4^+ form using cation-exchange resin.

Synthesis of m-Nitrobenzyl Triphosphate. A modified procedure of Davisson et al. (*9*) was used to synthesize nucleotidylated *m*-nitrobenzyl alcohol. To a solution of 1 mmol of *m*-nitrobenzyl bromide in 1 mL of anhydrous CH_3CN was added 1.5 eq of dry tetrakis(tetra-*n*-butylammonium) ATP. The solution was stirred for 6 h under nitrogen. The progress of the reaction was monitored by the disappearance of *m*-nitrobenzyl bromide ($R_f = 0.75$) using a TLC silica plate (Aldrich) with pet. ether/ether (1:1) as the mobile phase. The solution was diluted with distilled H_2O and loaded on a DEAE-Sephadex A25 (HCO_3^- form) column (5 cm × 20 cm) equilibrated with 0.3 M TEAB, pH 7.6. Elution was accomplished with a 2 L linear gradient of 0.2 to 0.9 M of TEAB, pH 7.6. TEAB was removed at 25 °C by repeated washes with 50% methanol on a rotary evaporator under vacuum. $NaIO_4$ degradation followed by base hydrolysis at 50 °C was performed on the nucleotidylated *m*-nitrobenzyl alcohol (*10*). The filtered solution was diluted with distilled H_2O and chromatographed on a DEAE Sephadex A 25 (HCO_3^- form) column with a 2 L linear gradient of 0.3 to 0.9 M TEAB, pH 7.6. After removal of TEAB, the sodium salt of *m*-nitrobenzyl triphosphate was obtained by eluting through a SP Sephadex C25 (Na^+ form) column. The overall yield of this procedure was 55%. ^{1}H NMR (200 MHz, D_2O): 8.17 ppm (1H, s, Ar), 8.03 ppm (1 H, d, $J = 8.0$ Hz, Ar), 7.71 ppm (1H, d, $J = 7.8$ Hz, Ar), 7.45 ppm (1H, apparent t, Ar), 4.97 ppm (2H, d, $J_{H-\alpha P} = 7.6$ Hz, methylene group). Decoupled ^{31}P NMR (161.9 MHz, D_2O pD = 8.3, external ref 85% phosphoric acid): −5.45 ppm (γ-phosphorus, d, $J_{\gamma-\beta} = 19.5$ Hz), −10.8 ppm (α-phosphorus, d, $J_{\alpha-\beta} = 19.5$ Hz), −21.1 ppm (β-phosphorus, apparent t). Negative ion MALDI-TOF mass spectrometry of *m*NBTP gave *m*/*z* 391.9 $(M - H)^-$.

Purification of KNTase.[2] The thermostable KNTase mutant, D80Y (TK1), was overexpressed in the *Escherichia coli* strain JM109(DE3) containing the expression plasmid pALT/TK1. The cells grown at 37 °C in LB medium with 100 μg/mL of tetracycline were induced ($OD_{600} = 1.2$) with 0.5 mM IPTG, harvested by centrifugation after 4 h of induction and frozen as pellets in liquid nitrogen. All purification procedures were carried out at 4 °C. The frozen cells were suspended in 50 mM triethanolamine and 1 mM EDTA, pH 7.5, to which had been added 1 mM PMSF, 52 mg/L of TLCK, 2.3 mg/L leupeptin, 1 mg/L pepstatin A, 20 mg/L soybean trypsin inhibitor, and 1.6 mg/L aprotinin. The cells were broken by sonication, and the debris was removed by centrifugation. Streptomycin sulfate was added to the supernatant to a final concentration of 1%. The supernatant obtained by centrifugation was dialyzed for 4 h against 20 mM triethanolamine and 0.1 mM PMSF. After ultracentrifugation the supernatant was loaded at 2 mL/min on a Q Sepharose FF column (5.0 × 23 cm). After washing the column with 20 mM NaCl, 20 mM triethanolamine, pH 7.5, the enzyme was eluted with a linear gradient of 4 L from 20 to 600 mM NaCl in 20 mM triethanolamine, pH 7.5. KNTase emerged at approximately 390 mM NaCl and was pooled based on SDS−PAGE analysis of the column fractions. Ammonium sulfate was added to a final concentration of

[2] The purification procedure of KNTase was developed by Dr. J. L. Vanhooke, Department of Biochemistry, University of Wisconsin—Madison.

1.0 M to this solution which was then loaded on a Butyl Sepharose 4 FF column (2.5 × 17 cm) equilibrated with 20 mM triethanolamine, 1.0 M ammonium sulfate, pH 7.5. A linear gradient from 1.0 to 0 M ammonium sulfate of 900 mL was applied. KNTase emerged roughly at 570 mM ammonium sulfate and was again pooled based on SDS−PAGE analysis of the column fractions. The enzyme was then precipitated with ammonium sulfate at 80% saturation. The pellet was resuspended with 20 mM triethanolamine, pH 7.0, with 0.04% sodium azide and dialyzed against the same buffer. The solution was concentrated to <9 mL by ultrafiltration in an Amicon stirred cell over a YM30 membrane and divided in three volumes of ∼3 mL each. Each aliquot was chromatographed on a tandem setup of two 2.5 × 91 cm columns of Sephacryl S200HR equilibrated with 20 mM triethanolamine, pH 7.0, with 0.04% sodium azide. KNTase was eluted with the same buffer and was again pooled based on SDS−PAGE analysis of the column fractions. Protein concentrations were determined using the BCA protein assay (Pierce) and the enzyme purity was determined to be greater than 95% by SDS−PAGE gel. The enzyme was stored at −80 °C at pH 7.0.

Assay of Kanamycin Nucleotidyltransferase and pH Profiles. The activity of kanamycin nucleotidyltransferase was assayed using a modified coupled enzyme assay described by Van Pelt and Northrop (*11*). The enzymatic reaction was followed at 340 nm by the increase in the rate of production of NADPH. Assay reactions were run in triplicate. The reaction was run at 25 °C in 50 mM buffer, 10 mM $MgCl_2$, 1 mM DTT with 0.2 mM UDP-glucose, 0.2 mM βNADP, and 0.2 μM glucose-1,6-bisphosphate. Sodium acetate buffer was used at pH 5.0, MES at pH 6.0, PIPES at pH 7.0, HEPES at pH 8.0, and CHES at pH 9.0. The concentrations of the coupling enzymes used were 2 units/mL phosphoglucomutase, 1 unit/mL glucose-6-phosphate dehydrogenase, and variable concentrations of UDP-glucose pyrophosphorylase from 4 unit/mL at pH 9.0 to 10 unit/mL at pH 5.0. When the KanA concentration was kept at 0.1 mM, the ATP or *m*NBTP concentration was varied from 0.1 to 0.7 mM for pH 5.0, from 0.1 to 1.0 mM for pH 6.0 and 7.0, and from 0.2 or 0.4 mM to 1.3 or 1.5 mM for pH 8.0 and 9.0. With *m*NBTP or ATP held constant at 0.5 mM, the concentrations of KanA was varied from 0.01 to 0.1 mM at pH 6.0. The kinetic constants were obtained by fitting the data to eq 1 using the program HYPER (*12*).

$$v = VA/(K + A) \quad (1)$$

Enzymatic Syntheses and Purifications of KanA-AMP and KanA-mNBMP. KanA-AMP and KanA-*m*NBMP were synthesized in 50 mM MES at either pH 6.0 or pH 5.7 in the presence of 1mM DTT, 10 mM $MgCl_2$, 1.5 mM ATP, or *m*NBTP and 1.0 mM KanA, 34 unit/mL and 855 unit/mL of TK1, respectively, as well as 8 unit/mL of inorganic pyrophosphatase. The reaction was followed by HPLC using a Vyadac 302IC4.6 column (4.6 mm × 250 mm) with buffer A from 0 to 3 min. From 3 to 18 min a gradient was applied from buffer A to buffer B for the ATP reaction and from buffer A to buffer C for the *m*NBTP reaction. Buffer A was 0.05 M K_2HPO_4/KH_2PO_4 (molar ratio 1:1) adjusted to pH 2.85 with acetic acid. Buffers B and C were, respectively, 0.25 and 0.3 M K_2HPO_4/KH_2PO_4 (molar ratio 1:1) adjusted to pH 2.93 with acetic acid. At 2 mL/min, KanA-*m*NBMP and KanA-AMP elute at 1.6 min, ATP at 10 min and *m*NBTP at 16 min. The reaction was stopped by filtration of the enzymes with a PM10 Amicon filter. The modified aminoglycosides were purified with a column of C25 SP Sephadex (NH_4^+ form) using a gradient from 0.1 to 0.3 M ammonium acetate, pH 8.3 (*13*). The separation between KanA and the modified KanA was monitored by analyzing the fractions with absorbance at 254 or 270 nm with a TLC silica plate (Aldrich) using the solvent system butanol/ethanol/chloroform/ammonia (4:5:2:8) (*14*). Aminoglycoside compounds were visualized by ninhydrin spray and UV. KanA has a lower R_f value (0.31) than that of KanA-AMP (0.45) or KanA-*m*NBMP (0.46). KanA-AMP was precipitated in ethanol at −20 °C, while ammonium acetate stayed in solution. The ammonium acetate was removed from the KanA-*m*NBMP pooled fractions by repeated rotary evaporation. Negative ion MALDI-TOF mass spectrometry of KanA-*m*NBMP gave *m*/*z* 698.1 $(M - H)^-$. Positive ion MALDI-TOF mass spectrometry of KanA-AMP gave *m*/*z* 814.0 $(M + H)^+$.

NMR Spectroscopy. Samples were lyophilized, prepared in D_2O, and adjusted to pD 6.8 unless otherwise noted. All ^1H, ^{13}C, and ^{31}P NMR spectra were acquired on a Bruker DMX-500 spectrometer at 300 K except those from HMQC (*15*) (Varian UnityPlus-500), DEPT for KanA and KanA-AMP (Bruker AC+ 300), and ^{31}P NMR for *m*NBTP (Bruker DMX-400) experiments. Standard pulse sequences were used for all experiments. Proton and carbon spectra were referenced to TSP: phosphorus spectra were referenced to an external standard of 85% phosphoric acid. All chemical shifts are reported in parts per million.

^1H NMR spectra were acquired with spectral widths of 6−7 kHz in 64K data points and 32−64 scans with relaxation delays of 3 s. The acquisition time was 4−5 s. $^1H-^1H$ DFCOSYPS (*16*) experiments were performed with pulse widths of 45° and spectral widths of 7.5 kHz. The acquisition time was 0.27 s. Spectra were acquired with 16 scans/increment in 4K × 2K data points. Processing included zerofilling to 4K × 4K data points and applying a shifted sine-bell squared window function in both dimensions. 1D TOCSY (*17*) experiments were run with mixing times of 20, 55, and 61.2 ms. These experiments were performed over a 10 kHz spectral width with 8K data points and 1024 scans. The acquisition time was 0.82 s. A selective 180° pulse was applied to desired proton. Processing included exponential multiplication (LB = 0.1 Hz). Prior to 1D NOE difference experiments, samples were purged with helium. Spectra were acquired over 7.5 kHz spectral width in 16K data points with 256 scans. The acquisition time was 1.09 s. The data were zerofilled to 32K and exponential multiplied (LB = 0.3 Hz).

^{13}C NMR were acquired with the noted spectrometer over a 28 kHz spectral width in 32K data points and 10000−16000 scans. DEPT135 (*18*) spectra were acquired over same spectral width in 32K data points and 512 scans. The FIDs were processed by exponential multiplication (LB = 2.5 or 3 Hz) and zerofilled to 64K data points. The $^1H-^{13}C$ HMQC (*19*) experiment was acquired over 8 kHz in 2K data points and over 22.6 kHz spectral width in 512 data points. Each increment contained 16 scans. After zerofilling to 2K × 1K data points, a shifted sine-bell window function was applied in both dimensions. The $^1H-^{13}C$ HSQC (*20*) experiment was taken over 7.5 kHz for 4K data points and over 9.3 kHz

Table 1: Kinetic Parameters of KNTase[a]

substrate	K_m (mM)	k_{cat} (s^{-1})	k_{cat}/K_m ($s^{-1}\,\mu M^{-1}$)
Mg-ATP	0.22 ± 0.06	1.3 ± 0.1	$(6 \pm 1) \times 10^{-3}$
Mg-*m*NBTP	0.29 ± 0.07	0.010 ± 0.001	$(35 \pm 5) \times 10^{-6}$

[a] Kinetic parameters were determined at 25 °C and at pH 6.0 with 50 mM MES, 10 mM $MgCl_2$, and 0.1 mM KanA as described in the Experimental Procedures.

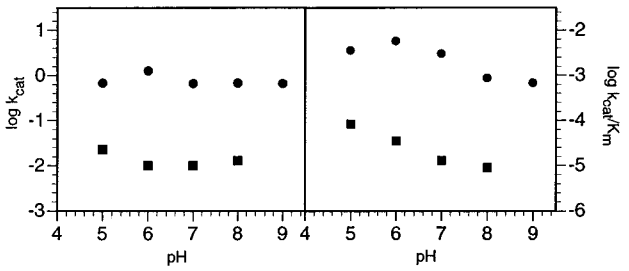

FIGURE 1: log k_{cat} and log k_{cat}/K_m versus pH profiles for the reactions of KNTase with ATP (●) and with *m*NBTP (■) were determined as described in the Experimental Procedures.

spectral width in 512 data points. The acquisition time was 0.27 s. Each increment contained 64 scans. A shifted sine-bell squared window function was applied in both dimensions. The $^1H-^{13}C$ HSQC-TOCSY (*21*) experiment was taken over 7.5 kHz for 4K data points and over 9.3 kHz spectral width in 256 data points. The acquisition time was 0.27 s. Each increment contained 48 scans. After zerofilling to 4K × 512 data points, a shifted sine bell squared window function was applied in both dimensions.

^{31}P NMR was acquired at 202.34 MHz over 8 kHz in 16K data points with a relaxation delay of 3 s. The acquisition time was 1.01 s. The FID was processed by exponential multiplication (LB = 2−3 Hz). $^1H-^{31}P$ COSY (*22*) spectra were taken over 10 kHz spectral width in 4K data points and over 600 Hz for 512 data points with 48 scans/increment. The acquisition time was 0.41 s. Processing included zerofilling to 4K × 1K data points and applying a shifted sine-bell squared window function in both dimensions.

RESULTS

Steady-State Kinetics. The steady-state kinetic constants, measured for the KNTase catalyzed reaction of KanA with ATP or *m*NBTP as the second substrate, are summarized in Table 1. In the KNTase reaction with *m*NBTP at pH 6.0 the k_{cat}/K_m and k_{cat} decreased by 176- and 138-fold respectively, compared to the reaction with ATP, while the K_m values for ATP and *m*NBTP were very similar.[3] The K_m values for KanA at pH 6.0 when the second substrate is ATP or *m*NBTP are 6 ± 1 and 18 ± 3 μM, respectively.

The pH dependencies of k_{cat} and k_{cat}/K_m for the reaction of KNTase with ATP are shown in Figure 1. The steady-state kinetic constants were not determined below pH 5.0 due to the instability of KNTase. The k_{cat} and k_{cat}/K_m versus pH plots for the reaction of KNTase with *m*NBTP are similar to the pH profiles for the reaction with ATP. They only differ in the pH optimum, which is 5.0 for the KNTase reaction with *m*NBTP and 6.0 for the reaction with ATP.

[3] The K_m value of UTP, dTTP, CTP, or GTP measured at pH 7.0 and with 0.5 mM KanA varies from 0.15 mM to 0.94 mM (*8*). The similarity of K_m values for all the triphosphate substrates is due to the lack of specific interactions between the nucleotide base and residues in the active site of kanamycin nucleotidyltransferase (*7*).

Table 2: ^1H and ^{13}C Chemical Shifts (ppm) of KanA and of the Kanamycin Moiety of Kan-AMP and Kan-mNBMP

		KanA		Kan-AMP		Kan-*m*NBMP	
ring	position	^1H (ppm)	^{13}C (ppm)	^1H (ppm)	^{13}C (ppm)	^1H (ppm)	^{13}C (ppm)
A	1′	5.55d	100.4	5.56d	99.4	5.53d	99.4
	2′	3.64dd	74.1	3.67dd	73.7	3.70dd	73.7
	3′	3.77t	75.2	3.91t	74.2	3.90t	74.3
	4′	3.37t	73.9	3.91m	77.5	3.94m	77.5
	5′	4.01td	71.8	4.15m	70.5	4.15m	70.7
	C6′ or $6'_x$	3.14dd	43.4	3.26dd	42.9	3.23dd	42.9
	$6'_y$	3.40dd		3.48dd		3.41dd	
B	1	3.19m	53.2	3.53m	52.9	3.32t	52.9
	C2 or 2a	1.49q	35.7	1.88q	32.5	1.61q	32.1
	2e	2.17dt		2.52dt		2.29dt	
	3	3.12m	51.4	3.49m	50.8	3.22t	50.8
	4	3.55t	85.6	3.83t	83.4	3.62t	82.8
	5	3.79t	76.7	3.90t	75.8	3.85t	75.9
	6	3.48t	89.1	3.74t	87.6	3.58t	87.4
C	1″	5.10d	103.0	5.15d	103.2	5.11d	103.3
	2″	3.72dd	73.0	3.96m	71.2	3.86dd	71.2
	3″	3.23t	57.5	3.52t	57.9	3.41t	57.9
	4″	3.52t	70.4	3.78t	68.5	3.65t	68.5
	5″	3.94dt	75.2	3.96m	75.4	3.95m	75.5
	6″	3.80m	62.9	3.81m	62.7	3.81m	62.7

Purification and Preliminary Characterization of Kan-AMP and Kan-mNBMP. Purification of the modified aminoglycosides was accomplished by cation exchange chromatography. Only one UV active peak eluted during the ammonium acetate gradient. KanA is more positively charged at pH 8.3 than the modified KanA; thus it has a longer retention time than the modified product and emerges after the UV active peak. KanA modified at the 4″ likely would elute with 4′ modified KanA, since both molecules have the same charges. Kan-AMP and Kan-*m*NBMP are both ninhydrin- and UV-sensitive, and both run differently on silica TLC from KanA ($\Delta R_f \approx 0.15$). The MALDI spectra confirmed that the compounds purified were Kan-AMP and Kan-*m*NBMP.

Assignment by NMR of the Products of the KNTase Reaction with ATP and mNBTP. Once we ascertained that the compounds isolated were Kan-AMP and Kan-*m*NBMP, we assigned the proton coupling constants and the proton and carbon chemical shifts for Kan-AMP and Kan-*m*NBMP at pD 6.8 on the basis of a multiplicity of one- and two-dimensional NMR spectra (Tables 2−4). Because of the pH dependence of ^1H NMR chemical shifts, assignments were obtained also for the ^1H and ^{13}C resonances of KanA independently of previous determinations (*23*−*25*). ^1H,^{13}C, DEPT135, COSY, HMQC, or HSQC techniques were used in assigning the majority of the ^1H and ^{13}C resonances for KanA, Kan-AMP, and Kan-*m*NBMP.

The ^{13}C resonances of ring B of the kanamycin moiety were assigned from the DEPT135 experiment and the HMQC correlation technique (Figure 2). From the correlations with the H-2a and H-2e in the COSY spectrum (Figure 3) it was shown that the chemical shifts of H-1 and H-3 overlap, as do those of H-4 and H-6. Other proton chemical shifts on ring B were readily assigned without recourse to additional experiments described below. All the protons and carbons of rings A and C except 3′ and 4′ of ring A were assigned

Table 3: $^{1}H-^{1}H$ Coupling Constants (Hz) of KanA and of the Kanamycin Moiety of Kan-AMP and Kan-*m*NBMP

ring	J_{x-x}	KanA (Hz)	Kan-AMP (Hz)	Kan-*m*NBMP (Hz)
A	$J_{1'-2'}$	3.9	4.0	4.0
	$J_{2'-3'}$	10	10.0	9.6
	$J_{3'-4'}$	9.5		9.0
	$J_{4'-5'}$	9.5		9.1
	$J_{5'-6'x}$	8.2	7.0	6.5
	$J_{5'-6'y}$	3.0	3.0	
	$J_{6'x-6'y}$	13.1	13.5	13.5
B	J_{1-2a}	12.5	12.5	12.5
	J_{1-2e}	4.3	4.0	4.0
	J_{2a-2e}	12.5	12.5	12.7
	J_{2a-3}	12.5	12.5	12.4
	J_{2e-3}	4.3	4.0	4.0
	J_{3-4}	9.7	9.7	9.6
	J_{4-5}	9.7	9.7	9.2
	J_{5-6}	9.7	10.5	9.2
	J_{6-1}	9.7	10.5	9.2
C	$J_{1''-2''}$	3.7	4.0	4.0
	$J_{2''-3''}$	10	10.1	10.7
	$J_{3''-4''}$	10	10.0	10.7
	$J_{4''-5''}$	10	10.0	10.0
	$J_{5''-6''}$	2.8	5.0	

Table 4: ^{31}P Chemical Shifts (ppm), $^{1}H-^{31}P$ and $^{13}C-^{31}P$ Coupling Constants (Hz) of Kan-AMP and Kan-*m*NBMP

Kan-AMP						
^{31}P ppm	$J_{H4'-P}$	J_{Cr5-P}	J_{Cr4-P}	$J_{C4'-P}$	$J_{C5'-P}$	$J_{C3'-P}$
−0.218	9.0	3.8	8.5	5.8	4.9	2.9tl
Kan-*m*NBMP						
^{31}P ppm	$J_{H4'-P}$	J_{Hm-P}	J_{Cb1-P}	J_{Cm-P}	$J_{C4'-P}$	$J_{C5'-P}$	$J_{C3'-P}$
0.606	7.2	8.9	7.7	5.0	5.9	4.3	2.5

respectively with the COSY and the HMQC experiments. Kan-AMP H-3′ and H-4′ have coincident chemical shifts and in the HMQC spectra (Figure 2) this resonance has a cross-peak with four carbons, two of which have very similar chemical shifts. The HMQC-TOCSY experiment distinguished between the carbons belonging to ring A (74.2 ppm, 77.5 ppm) and those of the other rings (75.8 ppm, 75.4 ppm). The final assignments of phosphorus coupled C-3′ and C-4′ are described later. The complete assignment of Kan-*m*NBMP was facilitated by the lack of both H-3′/H-4′ and H-2″/H-5″ overlaps and of the ribosyl protons. The identification of the protons for KanA was eased by the increased dispersion of the proton chemical shift in the region of 3−4 ppm.

Due to overlap of the proton resonances in the region of 3−4 ppm, not all proton chemical shifts and coupling constants could be assigned by both the 1D ^{1}H NMR spectra and the $^{1}H-^{1}H$ COSY. 1D ^{1}H TOCSY experiments (Figures 4 and 5) allowed the remaining assignments, except the connectivity of the middle (B) ring. A 180° pulse of 50 Hz bandwidth was used to selectively excite the anomeric H-1′ or H-1″ or the H-2a. The resulting magnetization was transferred around the ring so that all the proton resonances in the ring were excited. The resulting spectra were greatly simplified (Figures 4 and 5) showing protons from only one ring at a time. This enabled many chemical shift and coupling assignments, especially in the middle ring.

1D NOE difference experiments were performed on KanA-AMP and KanA-*m*NBMP to assign the connectivity of the aminocyclitol moiety to the other rings. The anomeric protons, H-1′ or H-1″, were irradiated in order to determine which proton, H-4 or H-6, of the middle ring was in close enough proximity to show an NOE over the glycosidic bond. For KanA-AMP, irradiating H-1′ caused inter-ring enhancements to H-4 and H-5 and irradiating H-1″ caused a strong inter-ring enhancements to H-6. For KanA-*m*NBMP, irradiating H-1″ led to enhancement of H-6. Irradiation of 1′ or 1″ of either compound also showed intra-ring enhancements to the adjacent proton, H-2′ or H-2″.

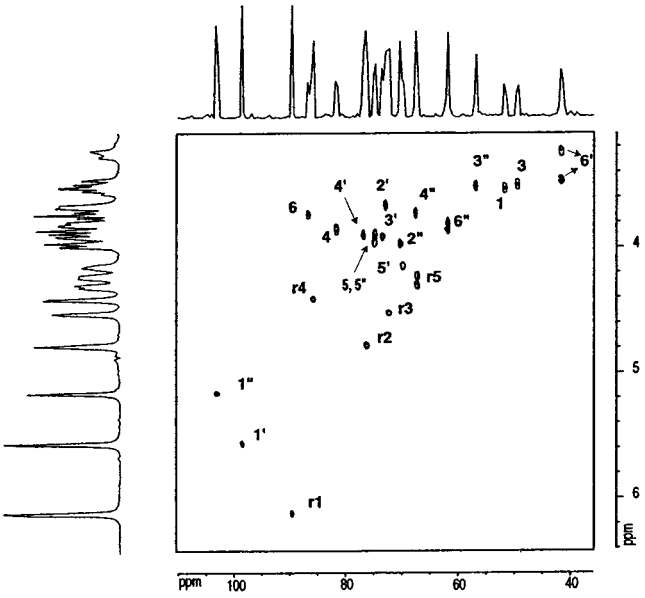

FIGURE 2: HMQC spectrum of Kan-AMP. The spectrum was acquired in D_2O at pD 6.8 at 300 K on a Varian UnityPlus-500 spectrometer as described in the Experimental Procedures.

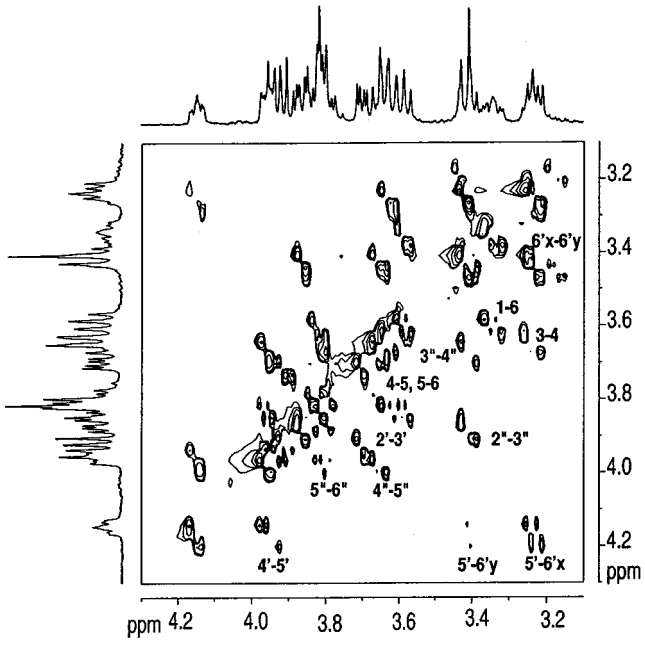

FIGURE 3: COSY 45 spectrum of Kan-*m*NBMP. The spectrum was acquired in D_2O at pD 6.8 at 300 K on a Bruker DMX-500 spectrometer as described in the Experimental Procedures.

Assignment by NMR of the Regiochemistry of the KNTase Reaction with ATP and mNBTP. ^{31}P NMR spectra of the products, KanA-AMP or KanA-*m*NBMP, of the KNTase reactions with KanA and ATP or *m*NBTP showed that only one regioisomer was produced in each case. The chemical

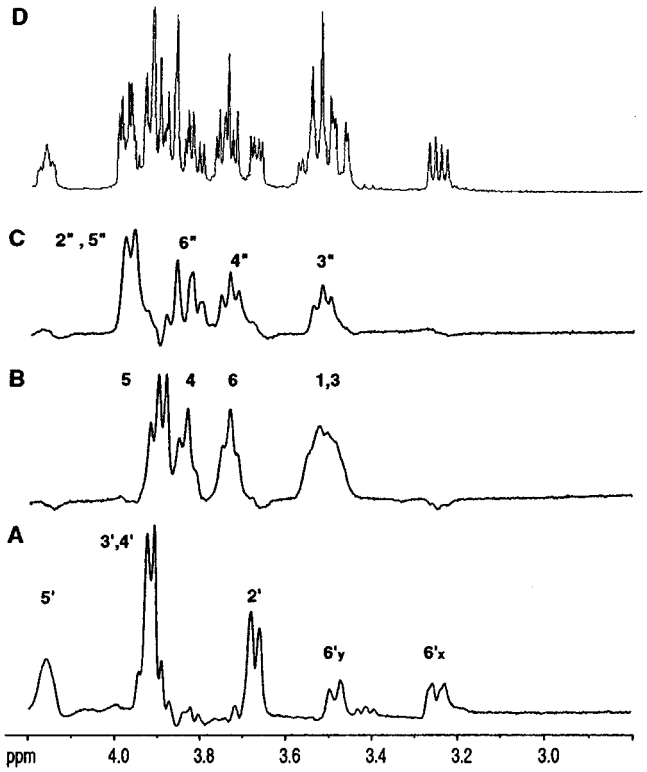

FIGURE 4: One-dimensional TOCSY and ^{1}H spectra of Kan-AMP. The spectra were acquired in D_2O at pD 6.8 at 300 K on a Bruker DMX-500 spectrometer as described in the Experimental Procedures. Spectra A, B, and C are, respectively, the 1D TOCSY spectra of ring A, B, and C of Kan-AMP. Spectrum D is the ^{1}H spectrum of Kan-AMP.

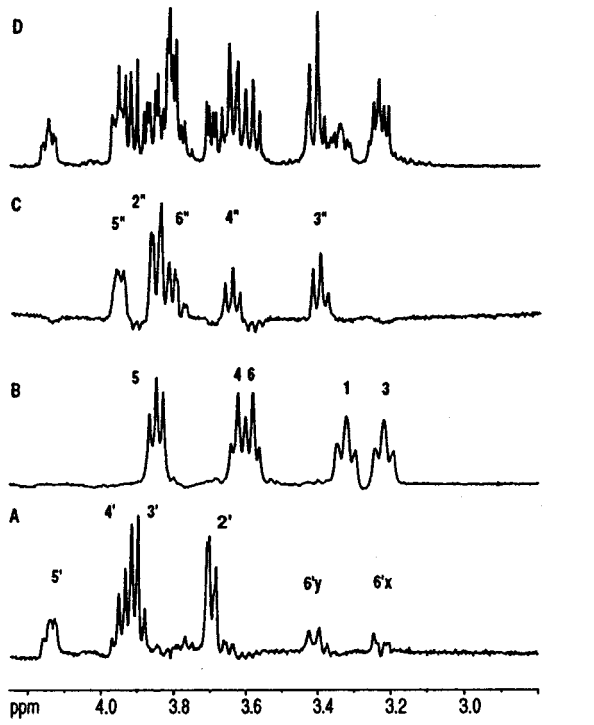

FIGURE 5: One-dimensional TOCSY and ^{1}H spectra of Kan-*m*NBMP. The spectra were acquired in D_2O at pD 6.8 at 300 K on a Bruker DMX-500 spectrometer as described in the Experimental Procedures. Spectra A, B, and C are respectively the 1D TOCSY spectra of ring A, B, and C of Kan-*m*NBMP. Spectrum D is the ^{1}H spectrum of Kan-*m*NBMP.

shifts, −0.22 and 0.61, respectively, reside in the region of phosphate diesters. The ^{13}C−^{31}P coupling constants (Table 4) determined from the ^{13}C spectra of the products provided the basis for the assignment of the site of modification. For KanA-*m*NBMP, the chemical shift with the largest ^{13}C−^{31}P coupling observed in the ^{13}C NMR spectra is C-4′, indicating that this site has been modified by the monophosphate diester. C-4′ was assigned from its 2D HMQC spectra. C-3′ and C-5′, each one more bond removed, have smaller ^{13}C−^{31}P couplings. Distinguishing between C-3′ and C-4′, both exhibiting ^{13}C−^{31}P coupling, of KanA-AMP could not be accomplished utilizing its 2D HMQC spectra because H-3′ and H-4′ have coincident chemical shifts. KanA-AMP's C-5′, which has a ^{13}C−^{31}P coupling, was routinely assigned. Because C-5′ has a phosphorus coupling and C-2′ does not, the carbon with the largest coupling was assigned to be next to C-5′, and the carbon with the smaller coupling to be next to C-2′. In addition to C−P coupling evidence for modification, C-4′ for both compounds is shifted downfield (+3.6), relative to C-4′ in the unmodified KanA. For both products, the proton chemical shift of 4′ showed the greatest difference (+0.54 and +0.57) from that of KanA. Since, in KanA-AMP, H-3′ and H-4′ have the same chemical shift and, in KanA-*m*NBMP, they are similar, ^{1}H−^{31}P COSY experiments were performed to determine the H−P coupling constant accurately. The coupling constants determined were in the range of typical $^3J_{PH}$ values.

Conformational Analysis. Although *m*NBMP- and AMP-substituents are sterically bulkier than the hydroxyl group of KanA, the conformation of ring A is unchanged in Kan-*m*NBMP and Kan-AMP from that of unmodified KanA. This is inferred from the fact that the $^3J_{H-H}$ coupling constants for this ring, and the other two rings, are similar for the three compounds. As for KanA, all the substituents, except for the two axial glycosidic bonds of rings A and C, are in equatorial positions and all rings are in chair conformations (*26*). The largest difference in coupling constant compared to that of KanA was observed for one of the methylene protons of the exocyclic aminomethyl group in ring A of Kan-AMP (Δ −1.2 Hz) and Kan-*m*NBMP (Δ −1.7 Hz) and may be due to a small change in the conformational equilibrium of the group. Chemical shifts and coupling constants are averages of the different conformations present. In KanA, the major conformer of this group has the C6′−N6 bond gauche with respect to the endocyclic O−C5′ bond and trans with respect to the C4′−C5′ bond. The change in coupling constants for the products indicates an increase in concentration of the gauche gauche conformer. This change may have occurred because of this 5′ substituent's proximity to the modified 4′ hydroxyl group.

The overall structure of KanA is presumed to be in dynamic equilibrium, in part shown by the absence of long-range NOEs (*24*). Short-range inter-ring NOEs were determined for the products of this reaction only to facilitate the assignment of the connectivity of the rings. The spectral data suggests the overall structures of Kan-AMP and Kan-*m*NBMP do not differ much from that of KanA. Some ^{13}C resonances, including some around the glycosidic bonds, are slightly more shielded than KanA resonances but they vary by the same magnitude for both products. The Kan-AMP proton resonances (except H-5) of the middle ring are on average shifted downfield 0.33 from those in KanA. To a smaller degree H-2″, H-3″, and H-4″ in ring C were also

shifted downfield (0.26). Deshielding of these protons could have occurred due to an increased contact with electronegative atoms or due to ring current effects of the adenine ring, depending on the conformation of the added substituent and its relationship to the rest of the compound. This effect was the only notable difference in the proton chemical shifts, except for the change due to phosphorylation of the H-4′ hydroxyl.

DISCUSSION

The increasing number of bacterial populations resistant to different antibiotics is jeopardizing the successful treatments of many bacterial infections (*1*). Thus, it is important to study the bacterial resistance mechanism in order to design new antibacterial drugs or derivatives of existing antibiotics whose bactericidal effect has been compromised. A thorough understanding of the reaction mechanisms of the aminoglycoside-inactivating enzymes implies the knowledge of the regiospecificity, kinetics, transition-state structure, three-dimensional structure of the resistance enzyme, and the interactions between the enzyme and the aminoglycosides. As a result, antibiotic modifying enzymes isolated from bacteria have been studied to find their mechanism of action. For instance kinetic, specificity and conformation studies have been reported for aminoglycoside 3′-phosphotransferase (*14*, *27*−*30*) and gentamycin 2″-nucleotidyltransferase (*13*, *31*−*33*), whereas until recently very little was known about KNTase.

KNTase modifies a variety of antibiotics that possess an equatorial 4′ or 4″ hydroxyl. The three-dimensional structure of KNTase with AMPCPP and KanA (*7*) shows a lack of interactions between active site residues and either ring A or ring C of KanA. The present results indicate that the noninteracting aminoglycoside ring must be ring C. Furthermore, the structure does not show interactions of KNTase with the adenine ring of AMPCPP (*7*). These facts explain the broad substrate specificity for the nucleotide and the aminoglycoside (*6*). Accordingly, *m*NBTP also proved to be a substrate in this reaction, and has a K_m similar to that of a natural substrate ATP (0.29 vs 0.22 mM). The slower rate of the reaction with *m*NBTP than with ATP indicates that the chemistry step is likely to be rate limiting.

Despite this broad substrate specificity, KNTase shows a strong preference for modification of ring A rather than ring C of KanA. The assignment of the site of modification as the 4′ hydroxy of ring A was based on the $^{13}C-^{31}P$ coupling constants determined from the ^{13}C spectra and full NMR assignment of KanA-AMP and KanA-mNBMP. The enzyme was shown to exclusively modify the 4′ hydroxyl even in the presence of an equatorial 4″ hydroxyl. The dinucleotidylated product or a nucleotidylated KanA at the 4″ position were not detected in the KNTase reaction. This result is unlike the reaction of aminoglycoside 3′-phosphotransferase with butirosin A, which has as products butirosin modified at the 3′ or at the 5″ and at both positions (*27*), but it is consistent with the aminoglycoside 3′-phosphotransferase catalyzed reaction of KanA (*14*). As previously shown, there are several active-site contacts between rings A and B in the crystal structure of KNTase (*7*). Ring A differs from ring C in the substitution of an aminomethyl group for a hydroxymethyl group and a hydroxyl group for an amino group. Studies with strategically deaminated KanA derivatives showed that the protonated amino groups are important for efficient catalysis with aminoglycoside 3′-phosphotransferase (*34*). The estimated binding energy due to a ammonium/enzyme residue was 6−11 kcal/mol. The placement of the ammonium groups may be similarly important here as shown by the regiospecificity.

In conclusion, the reaction of KNTase with KanA and with the slow substrate *m*NBTP is highly regiospecific for the 4′ position in the aminoglycoside, as it is with ATP. The ring conformations of the modified KanA products do not differ from the unmodified antibiotic. These results indicate that *m*NBTP may be utilized in the determination of the transition-state structure of the KNTase reaction through kinetic isotope effects (*35*). The information provided by this report should be useful in designing enzyme inhibitors able to prevent the deleterious reaction of KNTase on aminoglycoside antibiotics.

ACKNOWLEDGMENT

The authors thank Dr. Milo Westler for his assistance with NMR experiments and both Prof. John L. Markley and Dr. Eric J. Steinmetz for helpful comments.

SUPPORTING INFORMATION AVAILABLE

^{1}H, ^{13}C, $^{1}H-^{31}P$ COSY, MALDI-TOF, and remaining HSQC and COSY spectra of Kan-AMP and Kan-*m*NBMP. Also included are1D TOCSY spectra of KanA and the ^{1}H and ^{13}C assignments for the AMP- and the *m*NBMP-moieties. This material is available free of charge via the Internet at http://pubs.acs.org.

REFERENCES

1. Davies, J. E. (1991) in *Antibiotics in Laboratory Medicine* (Lorian, V., Ed.) pp 691−713, Williams & Wilkins, Baltimore, MD.
2. Davis, B. D. (1987) *Microbiol. Rev. 51*, 341−350.
3. Shaw, K. J., Ralter, P. N., Hare, R. S., and Miller, G. H. (1993) *Microbiol. Rev. 57*, 138−163.
4. Jacoby, G. A., Blaser, M. J., Santanam, P., Hachler, H., Kayser, F. H., Hare, R. S., and Miller, G. H. (1990) *Antimicrob. Agents Chemother. 34*, 2381−2386.
5. Schwotzer, U., Kayser, F. H., and Schwotzer, W. (1978) *FEMS Microbiol. Lett. 3*, 29−33.
6. Le Goffic, F., Baca, B., Soussy, C. J., Dublanchet, A., and Duval, J. (1976) *Ann. Microbiol. 127A*, 391−399.
7. Pedersen, L. C., Benninig, M. M., and Holden, H. M. (1995) *Biochemistry 34*, 13305−13311.
8. Chen-Goodspeed, M., Vanhooke, J. L., Holden, H. M., and Raushel, F. M. (1999) *Bioorg. Chem. 27*, 395−408.
9. Davisson, V. J., Davis, D. R., Dixit, V. M. and Poulter, C. D. (1987) *J. Org. Chem. 52*, 1794−1801.
10. Richard, J. P., and Frey, P. A. (1983) *J. Am. Chem. Soc. 105*, 6605−6609.
11. Van Pelt, J. E., and Northrop, D. B. (1984) *Arch. Biochem. Biophys. 230*, 250−263.
12. Cleland, W. W. (1975) *Methods Enzymol. 63*, 103−139.
13. Van Pelt, J. E., Mooberry, E. S., and Frey, P. A. (1990) *Arch. Biochem. Biophys. 280*, 284−291.
14. McKay, G. A., Thompson, P. R., and Wright, G. D. (1994) *Biochemistry 33*, 6936−6944.
15. Bax, A., Griffey, R. H., and Hawkins, B. L. (1983) *J. Magn. Reson. 55*, 301.
16. Marion, D., and Wuthrich, K. (1983) *Biochem. Biophys. Res. Commun. 113*, 967−974.

17. Bax, A., and Davis, D. G. (1985) *J. Magn. Reson. 65*, 355.
18. Doddrell, D. M.; Pegg, D. T., and Bendall, M. R. (1982) *J. Magn. Reson. 48*, 323.
19. Bax, A., and Subramaniian, S. (1986) *J. Magn. Reson. 67*, 565.
20. Bodenhaussen, G., and Rubin, D. J. (1980) *Chem. Phys. Lett. 69*, 185.
21. Lerner, L., and Bax, A. (1986) *J. Magn. Reson. 69*, 375−380.
22. Bain, A. D. (1988) *J. Magn. Reson. 77*, 125.
23. Eneva, G. I., and Spassov, S. L. (1991) *Spectrochim. Acta 47A*, 875−880.
24. Cox, J. R., and Serpersu, E. H. (1995) *Carbohydr. Res. 271*, 55−63.
25. Naito, T., Toda, S., Nakagawa, S., and Kawaguchi, H. (1980) in *Aminocyclitol Antibiotics* (Rinehart, K. L., and Suami, T., Eds.) pp 257−294, American Chemical Society, Washington, DC.
26. Koyama, G., and Iitaka, Y. (1968) *Tetrahedron Lett*. 1875−1879.
27. Cox, J. R., McKay, G. A., Wright, G. D., and Serpersu, E. H. (1996) *J. Am. Chem. Soc. 118*, 1295−1301.
28. Thompson, P. R., Hughes, D. W., and Wright, G. D. (1996) *Biochemistry 35*, 8686−8695.
29. Cox, J. R., and Serpersu, E. H. (1997) *Biochemistry 36*, 2353−2359.
30. McKay, G. A., and Wright, G. D. (1996) *Biochemistry 35*, 8680−8685.
31. Gates, C. A., and Northrop, D. B. (1988) *Biochemistry 27*, 3826−3833.
32. Gates, C. A., and Northrop, D. B. (1988) *Biochemistry 27*, 3834−3842.
33. Gates, C. A., and Northrop, D. B. (1988) *Biochemistry 27*, 3820−3825.
34. Roestamadji, J., Grapsas, I., and Mobashery, S. (1995) *J. Am. Chem. Soc. 117*, 11060−11069.
35. Gerratana, B., Frey, P. A., and Cleland, W. W. (2001) *Biochemistry 40*, 2972−2977

BI0025565